Author Manuscript

Visualization of integrin Mac-1 *in vivo*

Kihong Lim[*], **Young-Min Hyun**, **Kris Lambert-Emo**, **David J Topham**, and **Minsoo Kim**[*]

Department of Microbiology and Immunology, David H. Smith Center for Vaccine Biology and Immunology, University of Rochester, Rochester, NY, USA

Abstract

β2 integrins play critical roles in migration of immune cells and in the interaction with other cells, pathogens, and the extracellular matrix. Among the β2 integrins, Mac-1 (Macrophage antigen-1), composed of CD11b and CD18, is mainly expressed in innate immune cells and plays a major role in cell migration and trafficking. In order to image Mac-1-expressing cells both in live cells and mouse, we generated a knock-in (KI) mouse strain expressing CD11b conjugated with monomeric yellow fluorescent protein (mYFP). Expression of CD11b-mYFP protein was confirmed by Western blot and silver staining of CD11b-immunoprecipitates and total cell lysates from the mouse splenocytes. Mac-1-mediated functions of the KI neutrophils were comparable with those in WT cells. The fluorescence intensity of CD11b-mYFP was sufficient to image CD11b expressing cells in live mice using intravital two-photon microscopy. In vitro, dynamic changes in the intracellular localization of CD11b molecules could be measured by epifluorescent microscopy. Finally, CD11b-expressing immune cells from tissue were easily detected by flow cytometry without anti-CD11b antibody staining.

1. Introduction

Leukocytes circulate through blood vessels and lymphoid organs during normal condition and infiltrate the inflamed tissue upon infection or tissue damage. These processes are mediated by the dynamic interaction of integrins with their ligands, being governed by signals from various chemokines presented in the local tissues (Schall and Bacon, 1994; Klaus *et al*., 2007). Integrins, heterodimers of α- and β-subunits, are a large family of cell surface receptors that are responsible for cell adhesion and migration (Hynes, 2002). Among the three β integrin families (β1, β2 and β3), the β2 integrin family includes LFA-1 (CD11a/CD18) and Mac-1 (CD11b/CD18), the major integrins responsible for leukocyte trafficking (Hyun *et al*., 2010). Mac-1 is essential for intravascular crawling of innate immune cells such as neutrophils and monocytes (Phillipson *et al*., 2006; Sumagin *et al*., 2010). Blocking or deletion of Mac-1 dramatically inhibits the infiltration of innate immune cells to the

[*] To whom correspondence should be addressed: Kihong Lim, Ph.D., David H. Smith Center for Vaccine Biology and Immunology, University of Rochester Medical Center, 601 Elmwood Avenue, Box 609, Rochester, NY 14642, Kihong_Lim@urmc.rochester.edu, Phone: (585) 273-1435, and, Minsoo Kim, Ph.D., Department of Microbiology & Immunology, David H. Smith Center for Vaccine Biology and Immunology, University of Rochester Medical Center, 601 Elmwood Avenue, Box 609, Rochester, NY 14642, minsoo_kim@urmc.rochester.edu, Phone: (585) 276-3917, Fax: (585), 273-2452.

infected tissue and results in a significant defect in the clearance of the pathogens, indicating the importance of Mac-1 in innate immunity (Jiang *et al*., 1998; Phillipson *et al*., 2006).

Use of fluorescent cells has greatly facilitated cell tracking in live cell imaging. The fluorescent cells have been attained either by labeling the cells with an exogenous dye or fluorescent dye-conjugated antibodies, and by fluorescent protein expression from a transgene (Gebhardt *et al*., 2011; Lammermann *et al*., 2013). Specifically, the transgenic reporter mouse expressing a fluorescent protein in a cell-type specific manner has been an important tool in studying leukocyte behavior and localization in tissue using various imaging strategies such as intravital two-photon microscopy. In this study, we generated a knock-in (KI) mouse by inserting the monomeric yellow fluorescent protein (mYFP) gene at the end of the final exon of CD11b gene, which resulted in the KI mouse expressing the CD11b protein conjugated with mYFP within its carboxyl terminus.

2. Materials and methods

2.1. Mice

The CD11b-mYFP KI mouse strain was generated at the Gene Targeting and Transgenic Core facility of the University of Rochester (Rochester, NY, USA). The KI mouse was back-crossed to C57BL/6 for more than 10 generations. C57BL/6 mice were purchased from the National Cancer Institute (NCI), and all of the mice in this study were maintained in a pathogen-free environment within the University of Rochester animal facility. The animal experiments were performed in compliance with the protocols approved by the University Committee on Animal Resources at the University of Rochester.

2.2. Genotyping

The forward PCR primer was designed to anneal to the end of the last exon of the CD11b gene and the reverse primer to the region corresponding to 3' untranslated part of the CD11b mRNA (forward primer 5'-AGTACAAGGACATGATGAATGAAGCT-3' and reverse primer 5'-TGAGCACCTAAACCCTTGCAA-3'). PCR with this pair of primers amplifies 522 bp- and 1242 bp-long DNA fragments from WT and CD11b-mYFP KI alleles, respectively.

2.3. Epifluorescent microscopy

Fluorescence from splenocytes or neutrophils on a coverslip coated with 10 μg/ml recombinant mouse ICAM-1 (Sino Biological) or fibrinogen was captured using Nikon TE2000-E microscope. Neutrophils were purified from mouse bone marrow using an EasySep neutrophil enrichment kit (STEMCELL Technologies). To induce adhesion and migration, neutrophils were incubated with 2 μM fMLP (Sigma) at 37 °C during imaging.

2.4. Adhesion, phagocytosis, and transmigration assays

For adhesion assays, neutrophils were placed on an ICAM-1- or fibrinogen-coated glass slide with or without fMLP at 37 °C. Unbound cells were removed 15 min later and the number of bound cells was counted using microscopy. For phagocytosis assays, 100 μl of heparinized mouse blood was incubated with 100 μl of reconstituted pHrodo Red *S. aureus*

Bioparticles (Invitrogen) at 37 °C or 4 °C. After incubation for the indicated time, red blood cells were lysed and remaining white blood cells were harvested. Using fluorescence microscopy, phagocytic cells among CD11b-mYFP+ cells were counted based on their red fluorescence. WT CD11b+ cells were visualized by staining with FITC-conjugated anti-CD11b antibody (M1/70, Biolegend) before microscopy. For transmigration assays, neutrophils were placed inside a transwell insert (Thermo scientific, 12 mm diameter, 3 μm pore size) coated with ICAM-1 and the insert was placed in a receiver plate well filled with 1 μM fMLP-containing medium. After incubation for the indicated time at 37 °C, neutrophils in the receiver plate well were harvested and detected by flow cytometry.

2.5. Intravital two-photon microscopy (IV-TPM)

IV-TPM of mouse cremaster was previously described (Hyun *et al.*, 2012). For imaging of the trachea, a mouse was infected with influenza A virus (HKx31, 3×10^4 PFU), and at the indicated number of days post-infection, the mouse was deeply anesthetized using Avertin (2,2,2-tribromoethanol) and its trachea was exteriorized without bleeding. The exposed tracheal wall was opened by cross-sectionally half-cutting it, and an 18G blunt needle was inserted into the hall to restrict tissue movement and to enable the mouse to breathe through it. The mouse body was restrained on a custom-made stage, and both the body and trachea were warmed at 37 °C during the entire imaging session. To visualize neutrophils in the cremaster venules using intravital microscopy, 10 μg of FITC-conjugated anti-Ly6G antibody (1A8, Biolegend) was intravascularly injected before imaging. The blood vessels were visualized by Texas red-dextran (Sigma).

2.6. Image processes

Image processing and quantitative analysis of cell migration were performed using NIS (Nikon) and Volocity (PerkinElmer) software.

2.7. Flow cytometry

Single cell populations were prepared from the spleen or lung using a 40-μm strainer. One million of the cells were stained with 0.1 μg of anti-CD11b Alexa647 (M1/70, Biolegend), anti-CD45.2 Phycoerythrin (104, eBioscience), anti-CD3 allophycoerythrin (145-2C11, BD Bioscience), anti-Ly6G allophycoerythrin (1A8, Biolegend), anti-F4/80 Alexa647 (BM8, Invitrogen), anti-CD11c Alexa647 (N418, Biolegend), anti-Gr1 PerCP/Cy5.5 (RB6-8C5, BD Bioscience), anti-Ly6C Alexa 647 (HK1.4, Biolegend), and anti-CD115 APC (AFS98, Biolegend) at 4 °C for 45 min and analyzed using FACSCalibur (BD Bioscience).

2.6. Immunoprecipitation, silver staining, and Western blotting

Total lysates from splenocytes were prepared in PBS containing 1 % Triton X-100 and protease inhibitor cocktail (Roche). Immunoprecipitation was performed by incubating the lysates with agarose beads covalently immobilized with anti-CD11b antibody (M1/70), which were prepared using a Pierce Direct IP kit (Thermo scientific). The immunoprecipitated proteins or the total lysates were electrophoresed on a SDS polyacrylamide gel followed by silver staining or Western blotting using anti-GFP (sc-8334,

Santa Cruz biotechnology). This anti-GFP polyclonal antibody recognized YFP as efficiently as GFP.

3. Results

3.1. Generation of CD11b-mYFP knock-in mouse

We generated a knock-in (KI) mouse expressing CD11b conjugated with mYFP in its cytoplasmic C-terminal end (Fig. 1A). This KI mouse was back-crossed to C57BL/6 strain more than ten generations and did not exhibit any obvious defects in normal breeding. Selection of CD11b-mYFP KI mice strains was possible by simple genotyping by PCR of mouse genomic DNA. PCR primers were designed to flank the inserted mYFP gene so that the PCR product derived from CD11b-mYFP was approximately 700 bp larger than that from WT (Fig. 1B). Fluorescent microscopy and flow cytometry successfully detected YFP signal in neutrophils isolated from heterozygous and homozygous KI mice, but not in the WT cells (Fig. 1C). To confirm the expression and the integrity of the mYFP-conjugated CD11b protein molecule, immunoprecipitation of CD11b-mYFP was performed. Total lysates of spleens from CD11b-mYFP heterozygous (Het) or homozygous (Homo) mouse as well as a WT mouse were incubated with anti-mouse CD11b monoclonal antibody-immobilized beads, and the pull-downed fractions were analyzed using silver staining and Western blotting with anti-GFP antibody (Fig. 1D, left and middle). The results showed that the KI mouse expressed the CD11b-mYFP molecule at the expected molecular weight, which was approximately 27 kDa larger than that of unconjugated CD11b. Importantly, we did not detect any signs of CD11b-mYFP truncations in the total lysate, suggesting that all of the YFP fluorescence signals in this mouse strain originate from CD11b molecules (Fig. 1D, right).

CD11b is expressed mainly in innate immune cells so that the immune cell types expressing CD11b-mYFP were examined by flow cytometry of the splenocytes stained with various antibodies to cell type-specific surface markers. As expected, the innate immune cells including Ly6G^{+} neutrophils, F4/80^{+} monocytes/macrophages, and CD11c^{+} antigen presenting cells were YFP-positive, but CD3^{+} lymphocytes were not (Fig. 1E). Consistent with the heterogeneity of monocytes/macrophages, Gr1-positive cells expressed various levels of CD11b-mYFP.

3.2. Mac-1-mediated cellular functions in CD11b-mYFP KI mouse

Intracellular Mac-1 rapidly mobilizes to the plasma membrane upon stimulation (Sengelov *et al*., 1993). Consistently, neutrophils purified from both WT and CD11b-mYFP homozygous mouse showed a rapid increase in surface CD11b level at 30 min after stimulation with 2 μM fMLP, while total YFP intensity did not change in CD11b-mYFP expressing neutrophils (Fig. 2A). It is important to note that the surface expression level of Mac-1 was slightly lower in CD11b-mYFP KI neutrophils compared with WT (Fig 2B). However, Mac-1 mediated functions remained unperturbed in the KI homozygous mouse strain. First, neutrophils from CD11b-mYFP KI mice adhered to ICAM-1 and fibrinogen as efficiently as those from WT mice (Fig. 2C). Second, phagocytosis was equally effective both in KI and WT neutrophils (Fig 2D). Third, both WT and KI neutrophils migration

showed identical velocity, displacement, and meandering index on ICAM-1-coated surface (Fig. 2E). We further examined crawling of neutrophils in inflamed cremaster venules using intravital two-photon microscopy and confirmed that WT and KI neutrophils crawled similarly *in vivo* (Fig 2F). Finally, neutrophils from the KI and WT mice showed comparable chemotaxis toward fMLP through an ICAM-1-coated transwell (Fig 2G).

3.3. Fluorescence of CD11b-mYFP

We observed strong intracellular YFP fluorescence signal in non-adherent naïve neutrophils (Fig 3A). The intracellular CD11b remained during stimulation, while relatively weak but significant fluorescence appeared in the lamellipodia (Fig. 3A). We further examined CD11b-mYFP distribution during active migration of neutrophils on ICAM-1. Fig 3B and Movie 1 show that while a significant portion of CD11b-mYFP molecules were still detected inside the cell, the local intensity of YFP changed dynamically during the migration on ICAM-1. CD11b-enriched lamellipodia were often formed to a certain direction prior to cell migration following the direction.

Next, we performed intravital imaging to visualize CD11b-YFP$^+$ innate immune cells in the CD11b-mYFP KI mouse. IV-TPM of inflamed cremaster muscle vasculature showed a large number of YFP-positive cells adhering to the blood vessel wall and actively crawling (Fig. 3C and Movie 2). For imaging under more physiological conditions, we performed trachea imaging following influenza virus infection. The KI mouse was infected with influenza A virus, and its trachea was imaged 3 days later. The active migration of YFP-positive cells in the tracheal tissue was detected (Fig. 3D and Movie 3).

Finally, we analyzed infiltrated immune cells in the lung after influenza virus infection using flow cytometry. At day 4 post-infection, a large number of CD45.2$^+$ leukocytes infiltrated the infected lung, but not the uninfected lung (Fig 3E). Two major YFP$^+$ populations were detected; YFP^{High} cells were Ly6G$^+$ Gr1^{high} neutrophils, while YFP^{intermediate} cells were Ly6G$^-$Gr1$^+$ and F4/80$^+$CD115$^+$.

4. Discussion

Transgenic mouse strains expressing a fluorescent protein such as GFP, YFP or DsRed in a cell-type specific manner greatly facilitated studies for behavior and fate of a specific cell type (Lindquist *et al*., 2004; Stark *et al*, 2013; Ding and Morrison, 2013). To generate this type of reporter mouse, one of the pair of the cell type-specific gene is inactivated, and a reporter gene is expressed under its expression program. Instead of this strategy, we created a unique mouse strain expressing mYFP protein covalently conjugated with functionally intact CD11b molecules. The intensity of YFP-positive cells in this KI mouse was strong enough to identify and track individual immune cells through both *in vitro* and *in vivo* imaging.

The cell surface CD11b level of KI neutrophils was lower than that of WT neutrophils in both with and without stimulation. However, we did not observe any significant alterations in their functions. Our western blot assay further confirmed that there is no YFP cleavage from CD11b molecules. Therefore, YFP fluorescence was solely derived from the CD11b-

mYFP molecules and the YFP signals reflect CD11b expression and localization. In fact, we could detect that the local intensity of YFP was dynamically changed during active migration *in vitro*.

The use of CD11b-mYFP KI mouse has several advantages over anti-CD11b antibody staining for *in vivo* experiments. First, injection of an antibody (e.g. M1/70) to visualize CD11b+ cells may interfere Mac-1 integrin interaction with its ligands. Second, the antibody binding to its target cells may lead to depletion of the targeted cell population. Another benefit is real time monitoring of dynamic changes in Mac-1 distribution both in intracellular space and on cell surface. Importantly, however, we observed a significant decrease in the YFP fluorescence intensity after fixation using paraformaldehyde.

An additional use for this strain would be for cell type determination by flow cytometry. First, YFP can be read by a regular flow cytometer as it has excitation and emission spectra similar to GFP; thus, it is efficiently excited by a 488 nm laser and detected by the same bandpath filter for FITC and GFP. Second, CD11b has been useful in determining immune cell lineages such as CD11b+Gr1+ as a neutrophil or CD11b+Ly6G−CD115+ as a macrophage (Hanna *et al*., 2011). However, the pool of CD11b molecules is known to be mobilized rapidly to cell surface from the internal storage and is also actively internalized during cell stimulation (Sengelov *et al*., 1993: Bridgewater *et al*., 2012). Differential CD11b surface staining of the identical cell type may therefore reflect inconsistencies during different phases of stimulation. Therefore, the use of the CD11b-mYFP strain could help eliminate this variability.

In summary, we report the generation and the use of a novel CD11b-mYFP KI mouse strain, which provides a valuable tool for a broad range of imaging studies as well as cell identification.

Supplementary Material

Refer to Web version on PubMed Central for supplementary material.

Acknowledgement

References

Bridgewater RE, Norman JC, Caswell PT. Integrin trafficking at a glance. J. Cell Sci. 2012; 125:3695. [PubMed: 23027580]

Gebhardt T, Whitney PG, Zaid A, Mackay LK, Brooks AG, Heath WR, Carbone FR, Mueller SN. Different patterns of peripheral migration by memory CD4+ and CD8+ T cells. Nature. 2011; 47:216. [PubMed: 21841802]

Ding L, Morrison SJ. Haematopoietic stem cells and early lymphoid progenitors occupy distinct bone marrow niches. Nature. 2013; 495:231. [PubMed: 23434755]

Hanna RN, Carlin LM, Hubbeling HG, Nackiewicz D, Green AM, Punt JA, Geissmann F, Hedrick C. The transcription factor NR4A1 (Nur77) controls bone marrow differentiation and the survival of Ly6C− monocytes. Nat. Immunol. 2011; 12:778. [PubMed: 21725321]

Hynes RO. Integrins: bidirectional, allosteric signaling machines. Cell. 2002; 110:673. [PubMed: 12297042]

Hyun Y-M, Lefort CT, Kim M. Leukocyte integrins and their ligand interactions. Immunol. Res. 2009; 45:195. [PubMed: 19184539]

Hyun Y-M, Sumagin R, Sarangi PP, et al. Uropod elongation is a common final step in leukocyte extravasation through inflamed vessels. J. Exp. Med. 2012; 209:1349. [PubMed: 22711877]

Jiang N, Chopp M, Chahwala S. Neutrophil inhibitory factor treatment of focal cerebral ischemia in the rat. Brain Res. 1998; 788:25. [PubMed: 9554941]

Klaus L, Laudanna C, Cybulsky MI, Nourshargh S. Getting to the site of inflammation: the leukocyte adhesion cascade updated. Nat. Rev. Immunol. 2007; 7:678. [PubMed: 17717539]

Lammermann T, Afonso PV, Angermann BR, Wang RM, Kastenmuller W, Parent CA, Germain RN. Neutrophil swarms require LTB4 and integrins at sites of cell death *in vivo*. Nature. 2013; 498:371. [PubMed: 23708969]

Lindquist RL, Shakhar G, Dudziak D, Wardemann H, Eisenreich T, Dustin ML, Nussenzweig MC. Visualizing dendritic cell networks *in vivo*. Nat. Immunol. 2004; 5:1243. [PubMed: 15543150]

Luo BH, Carman CV, Springer TA. Structural basis of integrin regulation and signaling. Annu. Rev. Immunol. 2007; 25:619. [PubMed: 17201681]

Phillipson M, Heit B, Colarusso P, Lio L, Ballantyne CM, Kubes P. Intraluminal crawling of neutrophils to emigration sites: molecularly distinct process from adhesion in the recruitment cascade. J. Exp. Med. 2006; 203:2569. [PubMed: 17116736]

Schall TJ, Bacon KB. Chemokines, leukocyte trafficking, and inflammation. Curr. Opin. Immunol. 1994; 6:865. [PubMed: 7710711]

Sengelov H, Kjeldsen L, Diamond MS, Springer TA, Borregaard N. Subcellular localization and dynamics of Mac-1 (αMβ2) in human neutrophils. J. Clin. Invest. 1993; 92:1467. [PubMed: 8376598]

Stark K, Eckart A, Haidari E, et al. Capillary and arteriolar pericytes attract innate leukocytes exiting through venules and 'instruct' them with pattern-recognition and motility programs. Nat. Immunol. 2013; 14:41. [PubMed: 23179077]

Sumagin R, Prizant H, Lomakina E, Waugh RE, Sarelius IH. LFA-1 and Mac-1 define characteristically different intralumenal crawling and emigration patterns for monocytes and neutrophils in situ. J. Immunol. 2010; 185:7057. [PubMed: 21037096]
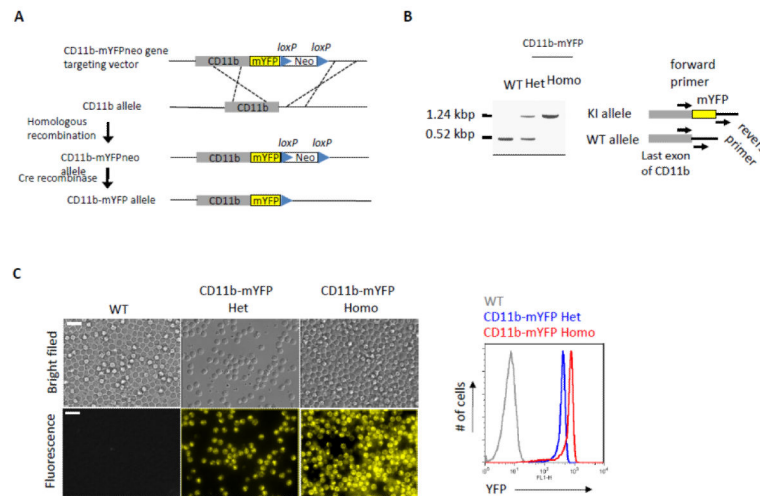
**Fig. 1. Generation of CD11b-mYFP Knock-in mouse**

(A) Scheme for generation of CD11b-mYFP knock-in (KI) mouse strain by homologous recombination and loxP/Cre recombinase system. Neo, neomycin-resistant gene. (B) Selection of the CD11b-mYFP mouse by genotyping. PCR with primers flanking mYFP insertion site (arrows on the right) amplified distinct DNA fragments from CD11b alleles of the indicated mouse strains. Het, CD11b-mYFP heterozygous; Homo, CD11b-mYFP homozygous. (C) YFP fluorescence from CD11b-mYFP KI mouse strains. Fluorescence signals of neutrophils from WT, heterozygous or homozygous CD11b-mYFP KI mouse was detected using epifluorescent microscopy (left panels) or flow cytometry (right graph). Scale bar, 20 μm. (D) Integrity of CD11b-mYFP molecule. CD11b proteins were purified by immunoprecipitating total lysates of splenocytes from the indicated mouse strains using an anti-mouse CD11b monoclonal antibody (M1/70) or its isotype control antibody, rat IgG2b (IgG). The immunoprecipitates or the total lysates were analyzed using silver staining (left) or Western blotting (center and right) using the indicated antibodies. (E) Specific cell types expressing CD11b-mYFP. Splenocytes from CD11b-mYFP KI mouse were co-stained with anti-CD45.2 and -Ly6G, -F4/80, -Gr1, or -CD11c antibodies, and analyzed by flow cytometry. The graphs on the left show YFP levels versus cell-specific surface markers of the CD45.2-positive populations. Numbers indicate the percentage of gated cell populations which are YFP-positive and the indicated surface marker-positive. The graph on the right shows the percentage of YFP- and the indicated surface marker-double positive cells from splenocytes (mean ± SEM, n = 3).

A

Staining: IgG / anti-CD11b / anti-CD11b
Stimulation: naive / naive / fMLP

WT

CD11b-mYFP Homo

YFP

CD11b

B

WT
CD11b-mYFP Homo

MFI

unstained

− fMLP   + fMLP

C

Adhesion

WT
CD11b-mYFP Homo

Bound (%)

ICAM
fMLP   −   −   +

Bound (%)

Fibrinogen   −   +   +
fMLP   −   −   +

D

Phagocytosis

WT
CD11b-mYFP Homo

Phagocytic CD11b+ cells (%)

Temperature (C0)   4   37   37
Time (hr)   3   1   3
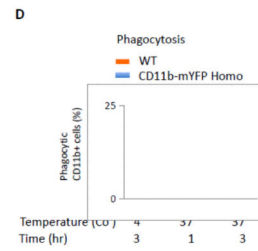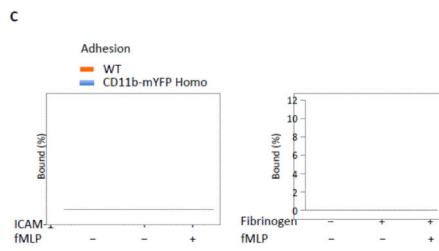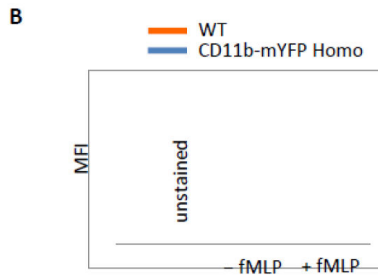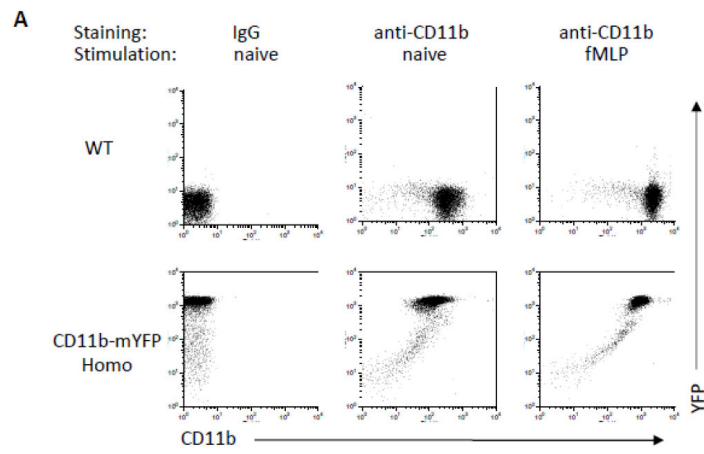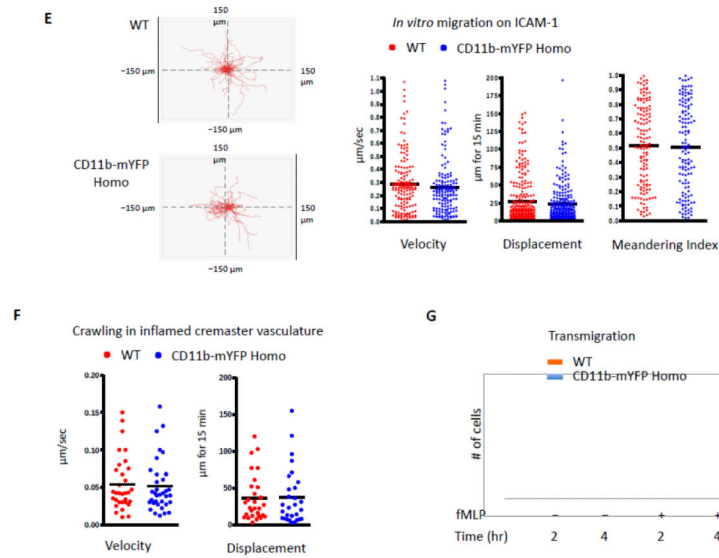
Fig 2. Mac1-mediated functions of CD11b-mYFP KI mouse
(A) Surface CD11b levels of neutrophils of CD11b-mYFP. Neutrophils purified from bone marrow of WT or CD11b-mYFP homozygous mouse were treated with or without fMLP and their surface CD11b levels were examined by flow cytometry following staining with an anti-CD11b antibody. (B) Quantification of surface CD11b levels measured in (A). MFI. Mean fluorescence intensity (mean ± SEM, n = 3). (C) Adhesion of CD11b-mYFP neutrophils. Neutrophils from WT or CD11b-mYFP homozygous mice were placed on ICAM-1- or fibrinogen-coated chamber in the presence or absence of fMLP and the number of bound cells were measured. The percentage of bound cells of the total input cells was presented (mean ± SEM, n = 3). (D) Phagocytosis of CD11b-mYFP+ cells. Blood from WT or CD11b-mYFP homozygous mice was incubated with pHrodo Red dye-conjugated *Staphylococcus aureus* bioparticles and the number of bioparticle-engulfed red-fluorescent CD11b-positive cells was measured using fluorescence microscopy. The percentage of phagocytic cells of the total CD11b+ cells was presented (mean ± SEM, n = 3). (E) *In vitro* migration of CD11b-mYFP neutrophils. Neutrophils from a WT or CD11b-mYFP homozygous mouse were allowed to migrate on an ICAM-1-coated coverslip in the presence of fMLP and cell migrations were recorded by videomicroscopy. Representative graphs of migratory tracks (left); comparison of velocity, displacement, and meandering index between WT and CD11b-mYFP (right). Points indicate individual cells combined from three independent assays. (F) *In vivo* crawling of CD11b-mYFP neutrophils. Intravital two-photon microscopy of neutrophils in fMLP-treated cremaster vasculature was performed. Neutrophils were visualized by intravascular injection of FITC-conjugated anti-Ly6G antibody before imaging. The graphs are the comparison of velocity and displacement between WT and CD11b-mYFP homozygous mice. Points indicate individual cells combined from three independent assays. (G) Transmigration of CD11b-mYFP neutrophils. Transmigration of neutrophils from WT or CD11b-mYFP homozygous mice through an ICAM-1-coated transwell insert toward 1 μM fMLP was measured at the indicated time points (mean ± SEM, n = 3).
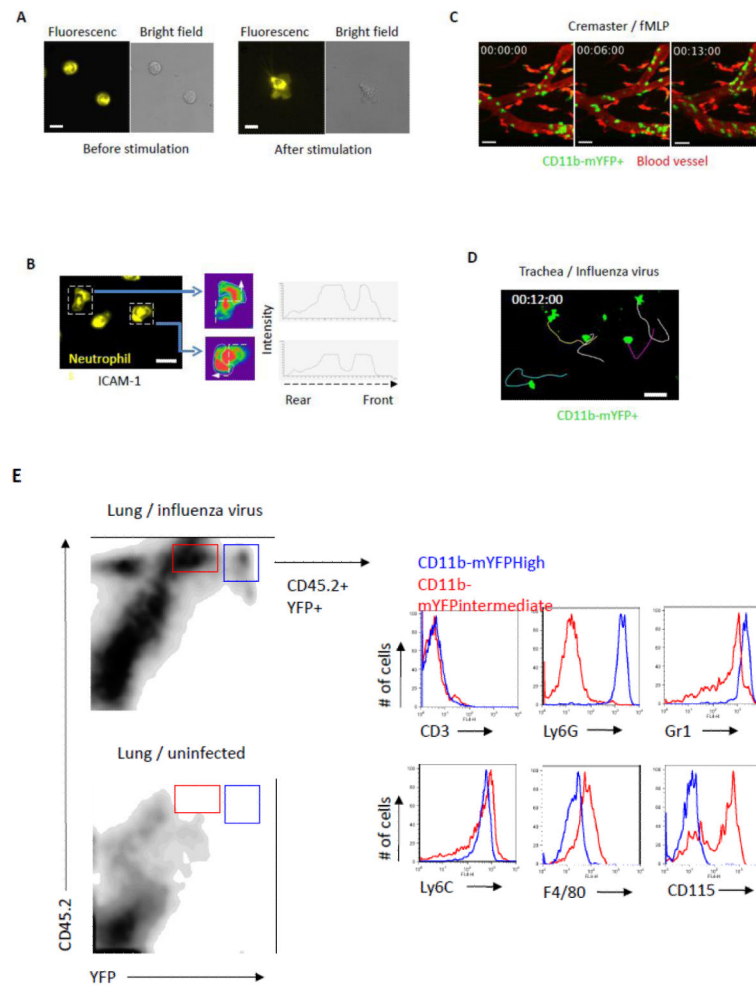
Fig. 3. Fluorescence of CD11b-mYFP+ cells

(A) Neutrophils from CD11b-mYFP homozygous mouse before and after activation on ICAM-1. Fluorescent and bright field images on the left show CD11b-mYFP neutrophils without stimulus at room temperature and those on the right show a CD11b-mYFP neutrophil at 37 °C in the presence of fMLP. (B) Neutrophils from CD11b-mYFP homozygous mouse were allowed to migrate on an ICAM-1-coated coverslip in the presence of fMLP and fluorescence of migrating neutrophils was recorded. A fluorescent image from each video was presented (left), and the YFP intensity over the cell body of the indicated neutrophils was alternatively shown in rainbow colors, highest (red) to lowest (purple), along the dotted line from the rear end to the front (center) or in graphs (right). The area marked with a white line in the center figures indicates lamellipodia. Scale bar, 10 μm. (C, D) CD11b-mYFP+ cell migration *in vivo*. Intravital two-photon microscopy was performed to observe migration of CD11b-mYFP+ cells in cremaster vasculature inflamed with fMLP (C) and in the trachea infected with influenza virus (D). Green, YFP-positive cells; Red, blood. Scale bar, 20 μm. Each curved line in (D) indicates the migratory track of the individual YFP-positive cell for 15 min. (E) CD11b-mYFP+ cell infiltration into infected tissue. CD11b-mYFP homozygous mouse was infected with influenza virus, and infiltrating leukocytes in the lung at day 4 post-infection were examined using flow cytometry. CD11b-

mYFP-positive leukocytes (YFP$^+$CD45.2$^+$) were divided into two groups based on YFP fluorescence intensity, YFP^{intermediate} (red) or YFP^{high} (blue), and the identity of each group was shown by staining with antibodies to the indicated cell type-specific surface markers.